New Evidence of Confinement Effects in Mesoporous Materials and the Definition of Confined Pitzer Acentric Factors

Philippe Trens,* Nathalie Tanchoux, Anne Galarneau, and François Fajula

Laboratoire de Matériaux Catalytiques et Catalyse en Chimie Organique, UMR 5618, CNRS/ENSCM/UM1, FR 1878 Institut Gerhardt, 8 rue de l'Ecole Normale, 34296 Montpellier Cedex 5, France

Received: March 29, 2005; In Final Form: June 20, 2005

In the present work, the corresponding states principle is proposed as a new approach to clarify the comparison between adsorption−desorption isotherms obtained on porous solids. The applicability of this principle at the capillary critical point in adsorption−desorption isotherms is demonstrated. Deviations of the Clausius−Clapeyron curves in reduced coordinates are interpreted in terms of polarizability, and those are perfectly correlated using analogous Pitzer acentric factors in confined environments. New acentric factors are proposed to take confinement effects in mesoporous materials into account. Enthalpic excesses during capillary condensation could be predicted, and those are supported by calorimetric experiments.

1. Introduction

The presence of a hysteresis loop is a common occurrence in the adsorption−desorption isotherms of gases over mesoporous adsorbents. The phenomenon is accounted for by the accepted mechanism of capillary condensation, in which pore filling occurs through the formation of a meniscus and its forward motion.[1] The formation of the meniscus is an activated process and takes place at a higher relative pressure than the desorption process, which only involves the rearward motion of the gas/vapor interface.

The values of relative pressure at which adsorption and desorption occur depend on the size of the pores and can be successfully calculated by modified forms of the Kelvin equation, taking into account the curvature of the pore surface.[2] The lowest closure point of the hysteresis loop corresponds to the pressure at which capillary desorption is completed. It was noticed early on that a threshold of relative pressure below which no hysteresis loop can be observed exists. This threshold depends on the nature of the adsorbate and was initially attributed to a tensional instability of the meniscus.[3]

The limit of stability of a liquid/gas interface is strongly reminiscent of the definition of a critical point. A large research effort has been devoted to the search for the critical properties of a confined fluid. Non-Localized Density Functional Theory (NLDFT) calculations allowed the adsorption and desorption branches of the isotherm to be calculated and a threshold value of temperature and pressure beyond which filling and emptying of a pore of a given size follow the same path to be determined.[4−6] It has been concluded that this capillary critical point does not correspond to the experimental limit at which no hysteresis can be observed. On the other hand, from theoretical studies, the limit value of the lowest closure point of the hysteresis loop has been interpreted as the point at which the grand canonical potential of the filled pore becomes higher than the potential of the empty pore.[7]

General correlations between this capillary critical point and other features of the isotherm have already been discussed.[8−10] For a given adsorbate, the capillary critical point strongly depends on the temperature and more precisely shifts toward higher relative pressures when the temperature increases,[11−13] while surface curvature effects have been evidenced to play an important role during the physisorption of gases in microporous solids and molecular sieves.[14] More recent research has attempted, with limited success, to correlate the pore critical temperature to the ratio between the size of the pore and the size of the molecules of adsorbate.[15] This study intends to investigate the principle of corresponding states as a new approach for comparing adsorption isotherms on mesoporous materials in order to clarify the general correlation between the pore critical temperature, the pore diameter, and the pore critical pressure.

2. Experimental Section

Sample Preparation and Textural Characterization. The adsorbent used in this work is an MCM-41 type silica prepared in the presence of hexadecyl trimethylammonium cations[16−17] accompanied by the swelling agent hexadecyl dimethylamine.[18] The gel mixture was heated in an autoclave reactor at 393 K for 48 h. The template was then eliminated by calcination under air flow (30 $cm^3 \cdot min^{-1}$) at 823 K for 5 h to generate the mesoporosity.

The temperature ramp was 1 $K \cdot min^{-1}$. The final material was characterized by nitrogen adsorption at 77 K and powder X-ray diffraction (XRD) (Figures 1 and 2, respectively). Nitrogen adsorption at 77 K on the MCM-41 material gives a type IV adsorption isotherm, with a steep capillary condensation uptake and a well-defined saturation plateau, typical of highly ordered mesoporous materials. The XRD pattern exhibits three reflections, which can be indexed according to a hexagonal (*P*6*mm*) structure. The [100] reflection (narrow, well defined) at 2.28° (2Θ) corresponds to a distance from one pore wall to an equivalent position in the adjacent wall of ∼3.9 nm.

The additional [110] and [210] reflections at higher 2Θ values indicate some substantial degree of ordering in the prepared material. The synthesized material is characterized by a specific surface area of ∼1200 $m^2 \cdot g^{-1}$, a pore diameter of 3.6 nm, and a pore volume of 0.95 $mL \cdot g^{-1}$.

* To whom correspondence should be addressed. E-mail: philippe.trens@enscm.fr. Fax: +33 467 163 470. Phone: +33 467 163 484.

10.1021/jp051591o CCC: $30.25
Published on Web 08/06/2005

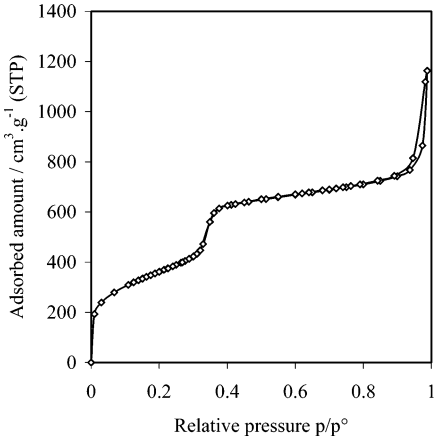

Figure 1. Nitrogen adsorption isotherm on the MCM-41 material at 77 K.

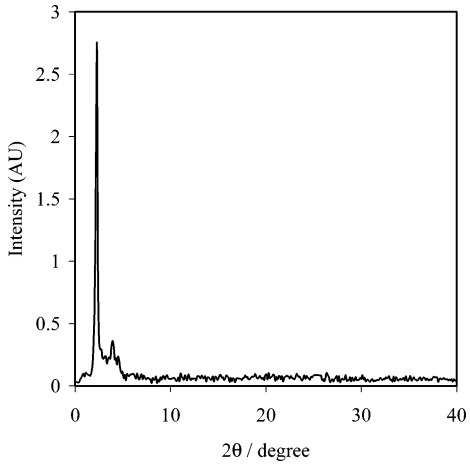

Figure 2. Powder X-ray diffractogram of the MCM-41 material.

Adsorption Studies. Sorption isotherms were determined using a home-built volumetric adsorption apparatus described elsewhere.[19] *N*-Hexane (Aldrich, purity >99.9%) and 1-hexene (Aldrich, purity >99%) were outgassed prior to use by freeze−thaw cycles under primary vacuum. A 150 mg portion of the mesoporous material was used for the adsorption experiments in the temperature range 273−333 K. The equilibrium time for each experimental data point ranged between 30 and 120 min depending on its location on the sorption curve.

To our data concerning the adsorption of *n*-hexane and 1-hexene but also nitrogen and oxygen, extra sorption isotherms were also collected from the literature. All materials used in the cited studies are mesoporous materials with a mean pore diameter of 3.6 nm (which may slightly vary, depending on the model used for the pore diameter determination), and the adsorbates used in those studies were either gases or vapors (argon,[9,20] xenon,[21] oxygen,[22,23] 2,2-dimethylbutane,[3] cyclopentane,[7] or benzene[3]).

3. Results and Discussion

Principle of Corresponding States. The adsorption isotherms of *n*-hexane or 1-hexene on the MCM-41 material at various temperatures are shown in Figure 3.

All adsorption isotherms belong to type IV according to the IUPAC classification: the curves exhibit a slight knee at low relative pressures (in the case of *n*-hexane, the adsorption curves almost follow a straight line which indicates its poor affinity for silica surfaces), followed by a steep capillary condensation step and a clear saturation plateau. The steepness of the capillary condensation indicates a very narrow pore size distribution (which is directly predicted by the Kelvin equation), confirming the high order suggested by the XRD diffractogram. The low uptakes observed during the adsorption on the saturation plateaus show that the material used is essentially mesoporous with a very small extent of external surface. As expected, saturation plateaus shift to low adsorbed amounts as the temperature increases, due to the variation of the density of sorbates for the different temperatures examined. The adsorption isotherms of *n*-hexane exhibit a hysteresis loop which shifts toward high relative pressure as the temperature increases, as already found for other systems, experimentally or by simulation theories.[24−28] In the case of 1-hexene, from 303 K upward, the adsorption isotherms are fully reversible in the range of temperatures studied.

For our experimental systems and also for those taken from the literature, a comparison between the different adsorption−desorption isotherms on different systems can be made.

Thus, a value of pressure, p_{cc}, and temperature, T_{cc}, can be extracted (cc standing for critical capillary) either as the lowest closure point of the hysteresis loop of each sorption isotherm, if any, or as the inflection point of the capillary condensation uptake when the sorption curve was fully reversible. All data are reported in Figure 4.

For each adsorbate/adsorbent system, the resulting data can be represented as a straight line, showing a continuous shift of the capillary critical point as the temperature increases. The relative position of the straight lines clearly depends on the boiling point and more interestingly on the critical temperature of the adsorbate under consideration. However, the influence of the temperature over each system is different, as suggested by the slopes of the curves. Plotting T/T_c versus $p_{cc}/p°$ did not clarify the situation (not shown here), so that on the basis of these first statements, no general correlation can be established.

A useful way of rationalizing those curves is to change the set of coordinates by using the principle of corresponding states which can be summarized by saying that gases at the same volume and temperature exert the same reduced pressure.[29] A reduced variable is obtained by dividing a real variable by its corresponding critical value. When plotting the same data in this new set of reduced variables, Figure 5 is obtained.

At first sight, the only improvement given by this chart is the fact that the curves have come closer to one another and are no longer sorted according to the boiling point of the different adsorbates. The different data can be perfectly fitted using logarithmic functions, but the relative position of the curves on the graph clearly appears to depend on the nature of the adsorbate (vapors higher than gases), which is apparently in contradiction with the principle of corresponding states because one would expect that all data lie on the same curve.

However, it is well-known that this principle works best for gases composed of spherical molecules but it fails when the molecules are polar or nonspherical which is the case here, for the organic vapors and some gases.

Pitzer suggested an empirical parameter, namely, the Pitzer acentric factor, ω, taking into account the nonsphericity of molecules and therefore their polarizability as a contribution for the nonideality of real gases.[30,31] Acentric factors have been defined as $\omega = -\log P_{vp,r}|_{T_r=0.7} - 1$ because the monatomic gases (Ar, Kr, and Xe) have $\omega \sim 0$ and, except for quantum gases (H_2, He, or Ne), all other species have positive values up to 1.5. To obtain values of acentric factors, ω, one needs the constants p_c and T_c and the value of vapor pressure at the reduced temperature $T/T_c = 0.7$. The reciprocal of T/T_c is the

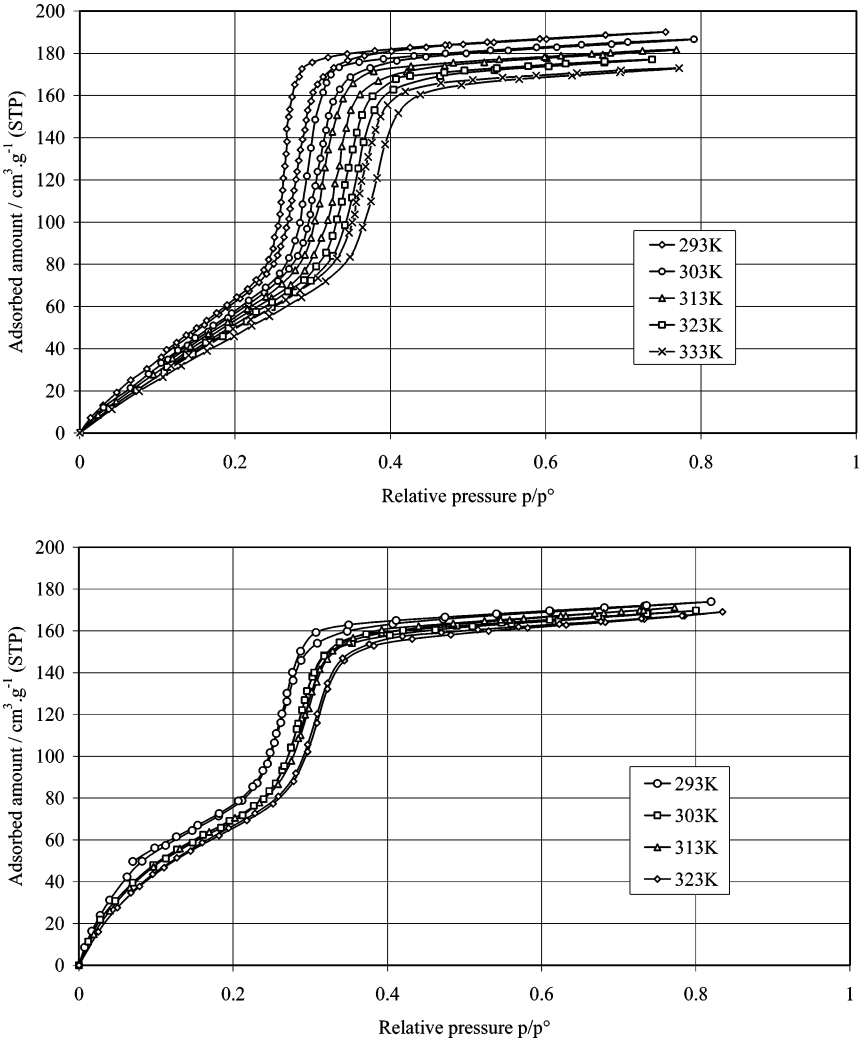

Figure 3. Sorption isotherms of *n*-hexane (top) or 1-hexene (bottom) over a 3.6 nm pore diameter MCM-41 material at various temperatures.

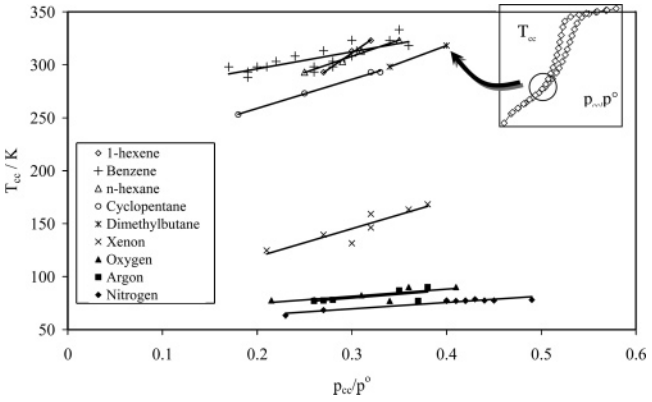

Figure 4. Closure points of hysteresis loops for various adsorptives on 3.6 nm mesoporous materials.

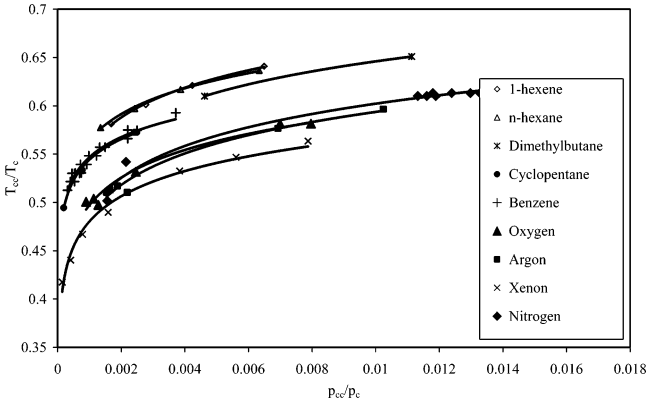

Figure 5. Closure points of hysteresis loops for various adsorbates on mesoporous materials using the principle of corresponding states.

X-axis of Figure 6, and the values of ω can be read for $1/T_r = 1.42$. The different values of the Pitzer acentric factor, ω, are summarized in Table 1 as well as the values of p_c and T_c.

These values of ω have been estimated experimentally in the past by plotting log p_r versus $1/T_r$, and many data can be found in the literature.[27−32]

This has been done here (Figure 6), in the case of gases or vapors in equilibrium with their corresponding adsorbed phase, at the capillary critical point. A Clausius−Clapeyron formalism has been employed to plot the data, as the definition of the acentric factor equation is strongly reminiscent of the Clausius−Clapeyron equation which can be written as

$$\frac{\mathrm{d} \ln p}{\mathrm{d} T} = \frac{\Delta_{vap} H}{RT^2}$$

It can be seen that for each adsorbate, pore critical data lie on an excellent linear correlation (some correlations have been omitted for clarity).

Furthermore, if these linear correlations are extrapolated toward higher pressure values, all lines pass through the point $T_{cc} = T_c$ and $p_{cc} = p_c$ (log $p_r = 0$ and $1/T_r = 1$), suggesting that

TABLE 1: Critical Data for the Different Adsorbates (ω^{cc} Data Are Derived from Figure 6)

	N_2	Ar	O_2	Xe	dimethylbutane	cyclopentane	benzene	*n*-hexane	1-hexene
p_c (atm)	33.9	48.98	50.43	58.4	30.9	45.08	48.98	29.3	31.3
T_c (K)	126.21	150.87	154.8	298.73	488.8	511.7	562.16	507.4	504.0
ω	0.04	-0.004	0.021	0.002	0.231	0.192	0.212	0.296	0.285
ω^{cc}	0.291	0.246	0.270	0.162	0.562	0.512	0.524	0.664	0.660

some correlation could exist between the limit lowest closure point of the hysteresis loop and critical points.

On the other hand, the values of ω (which can be named ω^{cc}) determined from Figure 6 are very different compared with those given by Pitzer (see Table 1). This difference is reminiscent of confinement effects often described in the literature. We suggest that the close presence of pore walls induces a strong curvature of the gas/adsorbed phase interface, which could induce a measurable modification of intermolecular interaction as compared to ideal systems. This is best demonstrated in Figure 7, by plotting the correlation between the Pitzer acentric factors of adsorbates and the values of ω^{cc} determined from Figure 6.

Apart from the data corresponding to xenon, all data lie on a straight line, which suggests that a principle of corresponding states exists for capillary critical points. This straight line does not pass through the origin which confirms the influence of confinement over the physicochemical properties of the gas phase at low pressures, even for gases as ideal as nitrogen or argon.

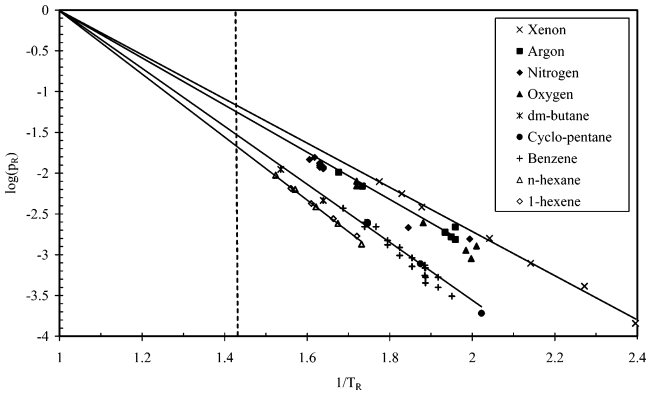

Figure 6. Lower closure points of the different sorption isotherm hysteresis loops using the principle of corresponding states and a Clausius−Clapeyron formalism.

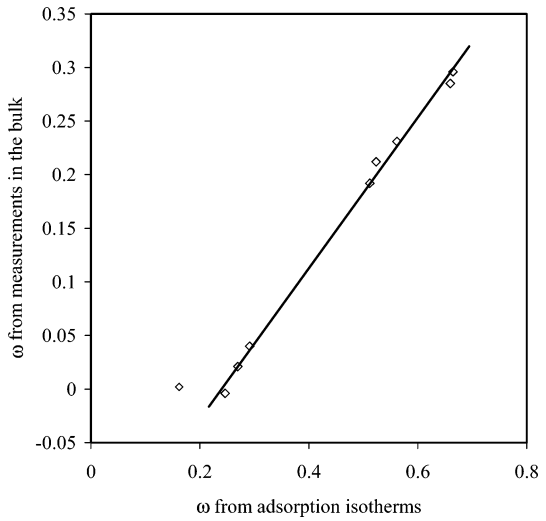

Figure 7. Comparison between published acentric factors, ω, and values derived from capillary critical points, ω^{cc}, for various fluids (from left to right: xenon, argon, oxygen, nitrogen, cyclopentane, benzene, dimethylbutane, *n*-hexane, and 1-hexene).

TABLE 2: Comparison of the Ratios "Confined Slope"/ "Bulk Slope" for the Different Systems

	ω	slope $\log(p_{cc}/p_c) = f(1/T_r)$	slope $\log(p_{eb}/p_c) = f(1/T_r)$	ratio
argon	−0.004	−2.88	−2.31	1.25
xenon	0.002	−2.71	−2.34	1.16
oxygen	0.021	−2.97	−2.39	1.24
nitrogen	0.04	−2.94	−2.42	1.21
cyclopentane	0.192	−3.59	−2.93	1.22
benzene	0.212	−3.69	−2.98	1.24
dimethylbutane	0.231	−3.65	−2.90	1.26
n-hexane	0.296	−3.74	−3.23	1.16
1-hexene	0.285	−3.88	−3.09	1.25

Furthermore, the slope of the line is lower than unity, indicating that the confinement effect is more effective for large molecules. This point suggests the influence of the pore size/ molecular diameter ratio which implies that the shift of ω to ω^{cc} is likely to be directly dependent on pore size. Therefore, after calibration for the gas of interest, a straightforward correlation between ω^{cc} and pore size can be established and used in a predictive way. The case of xenon (out of the line) may suggest that, in the temperature range where the adsorption isotherms of xenon have been measured, the physical state of the adsorbed phase has changed, which could induce changes in the equilibrium pressure.

Comparison between the Different Systems. It is of interest to gain information about the interaction involved at the gas/ adsorbed phase interface, and as pointed out above, Figure 6 is clearly reminiscent of Clausius−Clapeyron-like charts. The comparison of the curves obtained from capillary critical points with curves derived from condensation on flat surfaces is interesting by itself because the ratio of slopes can give information on intermolecular interaction in confined environments for the different adsorbing systems.

The curves corresponding to the condensation on flat surfaces have been derived using the classical Antoine equation to estimate the vapor pressure of adsorbates at various temperatures, according to the equation $\log[p_{vp}] = A - [B/(T + C)]$, where T is in kelvins and parameters A, B, and C depend on the vapor. The curves corresponding to the condensation at the capillary critical point are the same as those in Figure 6. The results for all adsorbates are reported in Table 2. The general observation that can be made is the difference between bulk condensation data and data for capillary condensation at the capillary critical point, which agrees with the difference between values of ω and ω^{cc}.

All ratios between the sets of slopes are situated at around 1.22, and it can be noticed that, for a given pore diameter, this ratio does not depend on the nature of the adsorbate nor on its geometry, as the same effect is present both for gases and organic vapors. On the other hand, this constant ratio probably depends on the pore size of the mesoporous adsorbents and the slight discrepancy between the observed ratios probably lies in the various models used for the determination of pore diameters.

It can be emphasized that from the enthalpy of condensation on a flat surface for any adsorbate, pressure values of capillary critical points can be easily estimated for a given temperature,

TABLE 3: Calorimetric Measurements for Different Adsorbing Systems with 3.6 nm Pore Diameter Materials ($\Delta_{cond}H_m$ and $\Delta_{cond}H_{bulk}$ Stand for the Enthalpy of Condensation in Mesopores and the Enthalpy of Condensation in the Bulk, Respectively)

adsorbate	ref	T (K)	T_r	$p/p°$	$\Delta_{cond}H_m$ (kJ/mol)	$\Delta_{cond}H_{bulk}$ (kJ/mol)	$\Delta H_m/\Delta H_{bulk}$
n-hexane	this work	303	0.596	0.22	−37.5	−31.6	1.19
1-hexene	this work	303	0.601	0.24	−36	−30.6	1.17
cyclopentane	Rathousky[7]	293	0.572	0.25	−35	−29	1.21
n-hexane	Jänchen[35]	303	0.596	0.23	−38	−31	1.23
acetonitrile	Jänchen[35]	303	0.553	0.41	−37	−32	1.16
water	Llewellyn[20]	292	0.451	0.52	−57	−44	1.30

provided the pore diameter is 3.6 nm and vice versa. In this study, we selected adsorption isotherms for several materials having pore diameters of 3.6 nm, and different ratios would have been likely found with different pore diameters. It can be anticipated that larger pore diameters would give lower ratios and, in the case of nonporous silica, the ratio should converge to unity.

The applicability of the principle of corresponding states can be generalized to confined systems and can also be used as a tool for the prediction of enthalpic excesses during adsorption processes. Hence, this effect evidenced at capillary critical points of adsorption isotherms can be generalized during the whole process of condensation of adsorbates in the mesopores of the materials.

Prediction of Enthalpic Excesses. The isosteric method has been used to determine the isosteric heat of adsorption versus coverage in the case of *n*-hexane or 1-hexene over a 3.6 nm pore diameter MCM-41 material.[33] Interpolations along the adsorption isotherm traces for obtaining identical adsorbed amounts have been performed by using polynomial functions.

This has been done for both branches of the sorption isotherms, and the isosteric heat of adsorption were found to be 1 kJ·mol^{-1} apart, which is in the range of the uncertainties given by microcalorimetric measurements. In Figure 8, the adsorption enthalpy of *n*-hexane has been plotted as a function of the fraction of pore filling.[26,34]

This isosteric enthalpic curve shows a typical adsorption process: the adsorption heat (a) steadily decreases in the low coverage part of the curve, in which a monolayer is being formed on the overall surface of the adsorbent; (b) remains at a virtually constant value during the pore filling; and (c) diverges when pore filling has been completed, as often observed. These classical features converge with published results.[25,28,35]

If we now focus on the capillary condensation process, it can be seen that the isosteric heat of condensation is higher than the enthalpy of condensation on a flat surface (−31.56 kJ·mol^{-1}). More precisely, throughout pore filling, the molar enthalpy of adsorption is remarkably constant at nearly −37.5 kJ·mol^{-1}, which corresponds to an enthalpic excess of 5.7 kJ·mol^{-1} as compared with the condensation enthalpy in the bulk. The ratio between the two values of condensation enthalpies is 1.19, which is consistent with the typical ratio found above.

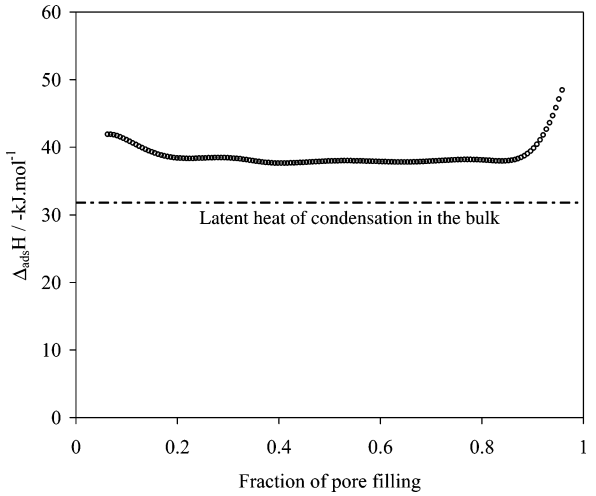

Figure 8. Isosteric heat of adsorption of *n*-hexane over MCM-41 at 303 K, derived from the isosteric method.

The same agreement is found with 1-hexene used as adsorbate (Figure 9). Furthermore, if we now compare condensation enthalpies in mesoporous materials from calorimetric results published in the literature with calculated bulk condensation enthalpies, the same agreement can be put forward (see Table 3).

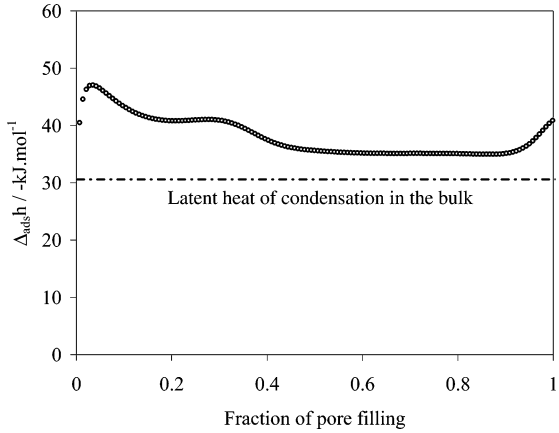

Figure 9. Isosteric heat of adsorption of 1-hexene over MCM-41 at 303 K, derived from the isosteric method.

4. Conclusion

The principle of corresponding states can be employed for predicting capillary critical points but also for predicting enthalpic excesses during capillary condensation processes. This method is general and can be used when adsorbing either gases or vapors. Furthermore, this method does not depend on the chemical nature of the surface of the pore wall, as different materials have been used (mineral oxides or carbons). New acentric factors determined from the sorption isotherms illustrate confinement effects which rule capillary condensation processes in mesoporous materials. Confined geometries must be seen as nanoreactors where classical equations of state of vapors do not apply. This is exemplified by the fact that empirical parameters such as Pitzer acentric factors do not lead to acceptable correlations between experimental data and expected physicochemical properties.

Clausius−Clapeyron equations allow the enthalpies of condensation to be determined from pressure and temperature data. They are not corresponding state laws. Nevertheless, they apply extremely close to the critical point, and therefore, it seems reasonable to explore their application to the lowest closure point of the hysteresis loop.[36] New systems are under investigation to generalize even further the use of the principle of corresponding states to confined environments, by testing materials

having smaller mesopores, and also different porous networks such as SBA-15 or MCM-48 materials.

References and Notes

(1) Gregg, S. J.; Sing, K. S. W. *Adsorption, surface area and porosity*, 2nd ed.; Academic Press: London, 1982; see also references therein.

(2) (a) Broekhoff, J. C. P.; de Boer, J. H. *J. Catal.* **1967**, *9*, 8; **1967**, *9*, 15.

(3) Burgess, C. G. V.; Everett, D. H. *J. Colloid Interface Sci.* **1970**, *33*, 611.

(4) Evans, R.; Marconi, U. M. B.; Tarazona, P. *J. Chem. Phys.* **1986**, *84*, 2376.

(5) Ball, P. C.; Evans, R. *Langmuir* **1989**, *5*, 714.

(6) de Keizer, A.; Michalski, T.; Findenegg, G. H. *Pure Appl. Chem.* **1991**, *63*, 1495.

(7) Rathousky, J.; Zukal, A.; Franke, O.; Schulz-Ekloff, G. *J. Chem. Soc., Faraday Trans.* **1995**, *91*, 937.

(8) Sonwane, C. G.; Bathia, S. K.; Calos, N. *Ind. Eng. Chem. Res.* **1998**, *37*, 2271.

(9) Machin, W. D. *Langmuir* **1994**, *10*, 1235.

(10) Thommes, M.; Kohn, R.; Froba, M. *Appl. Surf. Sci.* **2002**, *196*, 239.

(11) Morishige, K.; Nabuoka, K. *J. Chem. Phys.* **1997**, *107*, 6965.

(12) Machin, W. D. *Langmuir* **1999**, *15*, 169.

(13) Neimark, A.; Ravikovitch, P. I.; Grun, M.; Schuth, F.; Unger, K. K. *J. Colloid Interface Sci.* **1998**, *207*, 159.

(14) Derouane, E. G.; Andre, J.-M., Lucas, A. A. *J. Catal.* **1988**, *110*, 58.

(15) Morishige, K.; Fujii, H.; Uga, M.; Kinukawa, D. *Langmuir* **1997**, *13*, 3494.

(16) Grün, M.; Unger, K. K.; Matsumoto, A.; Tsutsumi, K. In *Characterisation of Porous Solids IV*; McEnaney, B., Mays, T. J., Rouquérol, J., Rodrigruez-Reinoso, F., Sing, K. S. W., Unger, K. K., Eds.; Royal Society of Chemistry: London, 1997.

(17) Ying, J. Y.; Mehnert, C. P.; Wong, M. S. *Angew. Chem., Int. Ed.* **1999**, *38*, 56.

(18) Sayari, A.; Yang, Y.; Kruk, M.; Jaroniec, M. *J. Phys. Chem. B* **1999**, *103*, 3651.

(19) Tanchoux, N.; Trens, P.; Maldonado, D.; Di Renzo, F.; Fajula, F. *Colloids Surf.* **2004**, *246*, 1.

(20) Llewellyn, P. L.; Schüth, F.; Grillet, Y.; Rouquerol, F.; Rouquerol, J.; Unger, K. K. *Langmuir* **1995**, *11*, 574.

(21) Machin, W. D.; Golding, P. D. *J. Chem. Soc., Faraday Trans.* **1990**, *86*, 171.

(22) Barrer, R. M.; MacLeod, D. M. *Trans. Faraday Soc.* **1954**, *50*, 980.

(23) Barrer, R. M.; McKenzie, N.; Reay, J. S. S. *J. Colloid Sci.* **1956**, *11*, 479.

(24) Franke, O.; Schulz-Ekloff, G.; Rathousky, J.; Starek, J.; Zukal, A. *J. Chem. Soc., Chem. Commun.* **1993**, 724.

(25) Branton, P. J.; Hall, P. G.; Sing, K. S. W.; Reichert, H.; Schüth, F.; Unger, K. K. *J. Chem. Soc., Faraday Trans.* **1994**, *90*, 2965.

(26) Ravikovitch, P. I.; Domhnaill, S. C. O.; Neimark, A. V.; Schüth, F.; Unger, K. K. *Langmuir* **1995**, *11*, 4765.

(27) Morishige, K.; Shikimi, M. *J. Chem. Phys.* **1998**, *108*, 7821.

(28) Qiao, S. Z.; Bathia, S. K.; Nicholson, D. *Langmuir* **2004**, *20*, 389.

(29) Guggenheim, E. A. *J. Chem. Phys.* **1945**, *13*, 253.

(30) Pitzer, K. S.; Curl, R. F. *J. Am. Chem. Soc.* **1955**, *77*, 3427.

(31) Reid, R. C.; Prausnitz, J. M.; Sherwood, T. K. *The properties of gases and liquids*, 3rd ed.; McGraw-Hill: New York, 1976.

(32) Pitzer, K. S.; Lippmann, D. Z.; Curl, R. F.; Huggins, C. M.; Petersen, D. E. *J. Am. Chem. Soc.* **1955**, *77*, 3433.

(33) Rouquerol, F.; Rouquerol, J.; Sing, K. *Adsorption by powders and porous solids*; Academic Press: San Diego, CA, 1999; p 203.

(34) Trens, P.; Tanchoux, N.; Maldonado, D.; Galarneau, A.; Di Renzo, F.; Fajula, F. *New J. Chem.* **2004**, *28*, 874.

(35) Jänchen, J.; Stach, H.; Busio, M.; van Wolput, J. H. M. C. *Thermochim. Acta* **1998**, *312*, 33.

(36) Guggenheim, E. A. In *Thermodynamics; An Advanced Treatment for Chemists and Physicists*; Macmillan Publishing: New York, 1960.